[P3]

P. Suvikunnas, J. Salo, L. Vuokko, J. Kivinen, K. Sulonen and P. Vainikainen, *Comparison of MIMO antenna configurations: methods and experimental results,* Helsinki University of Technology, Radio Laboratory, Report S 279, Espoo, Finland, June 2006, 27 p.

Helsinki University of Technology Radio Laboratory Publications
Teknillisen korkeakoulun Radiolaboratorion julkaisuja
Espoo, June 2006 REPORT S 277

COMPARISON OF MIMO ANTENNA CONFIGURATIONS: METHODS AND EXPERIMENTAL RESULTS

Pasi Suvikunnas Jari Salo Lasse Vuokko Jarmo Kivinen Kati Sulonen
Pertti Vainikainen

Helsinki University of Technology
Department of Electrical and Communications Engineering
Radio Laboratory

Teknillinen korkeakoulu
Sähkö- ja tietoliikennetekniikan osasto
Radiolaboratorio

Distribution:
Helsinki University of Technology
Radio Laboratory
P.O. Box 3000
FI-02015 TKK
Tel. +358-9-451 2252
Fax. +358-9-451 2152

ISBN 951-22-8229-1
ISSN 1456-3835

Otamedia Oy
Espoo 2006

Abstract

In this paper, methods for comparing multiple-input multiple-output (MIMO) antenna configurations using measured radio channels are considered. The expression of mutual information is factorized for giving better understanding on the ability of MIMO antenna systems to transfer signal power as well as to utilize parallel channels. Proper power normalization of channel matrices is shown to have profound impact on the ranking of especially directive MIMO antennas. It was found that the ability to transfer signal power from the transmitter to the receiver, instead of channel rank properties, dominates the antenna performance over a wide range of signal-to-noise-ratios. The highest performance differences between the antennas were found at low outage probability levels, especially in line-of-sight. It was also verified that the antenna systems utilizing two orthogonal polarizations are more robust for environmental variations but more sensitive to antenna orientation compared to the single polarization antenna systems both in eigenvalue dispersion and transferred signal power. At low outage probability levels the best performance was achieved with vertically polarized dipole antennas.

Table of contents

1 Introduction

The multiple-input multiple-output (MIMO) concept is the promising solution to increase spectral efficiency in wireless communication systems [1], [2]. There are three basic transceiver techniques a MIMO system can utilize: beam-forming, spatial diversity, and spatial multiplexing. The first two can also be used in the single-input multiple-output (SIMO) and the multiple-input single-output (MISO) systems, but the spatial multiplexing is possible only in the MIMO systems where several antennas are employed at both ends of the radio link. Spatial multiplexing refers to a transmission scheme where multiple data streams are transmitted in parallel over the radio channel. Spatial multiplexing increases data rate over the used signal bandwidth while spatial diversity increases the reliability of the signal [3], [4], [5]. The results of this paper are valid in both the diversity and the multiplexing systems. However, this paper is focused only for fixed-beam antennas, and hence, do not consider beam-forming systems.

The empirical antenna evaluation is not the new area of research among the more traditional systems like single-input single-output (SISO) and SIMO. Antenna evaluation problem has been considered for single antenna receivers e.g. in [6] and [7] or double antenna receivers e.g. in [8], [9], [10] and [11]. From antenna point of view an often-used optimality criterion of SISO systems is the average capability of the antenna to receive energy from the electromagnetic field defined by the mean effective gain (MEG) [6], [12]. Naturally, significant energy saving can be achieved if signal-to-noise-ratio (SNR) increases due to the reasonable antenna selection, which, in turn, increases the operating time of a communication device. However, the effect of antennas on the MIMO performance is not that well-known and systematically studied area. In the MIMO systems, multiple antenna elements are adopted at both ends of the link. This makes optimality criterion even more complex because it depends not only on the capability of a MIMO system to transfer signal power between the link ends, but also on the ability to utilize parallel spatial channels. The capacity of MIMO systems including the effect of the antennas has been considered e.g. in [13], [14], [15] and [16]. The polarization properties of the antennas used in MIMO systems have been investigated e.g. in [13] and [14].

Firstly, this paper proposes new practical figures of merit for empirical and systematical MIMO antenna comparison including SISO, SIMO and MISO systems as special cases. Secondly, the significance of the proposed figures of merit is validated by the actual antenna evaluation of some test antennas in three different signal propagation environments. The effect of antenna properties on the performance of MIMO systems is especially highlighted. It is verified how the received power depends on the normalization of channel matrix, and a novel normalization procedure is proposed. The measurement results of a 2 GHz wideband MIMO channel sounder [17] are utilized by using an experimental plane-wave based method (EPWBM) [7] [18] in the evaluation of the antennas. The EPWBM is the antenna evaluation method that is based on the combination of estimated directional channel distribution and the radiation patterns of antennas under test (AUTs).

The paper is organized as follows. The system model used is presented in Section II. Novel performance measures for the evaluation of MIMO antenna systems are discussed in Section III. The description of measurement system and measurement antennas is presented in Section IV. The MIMO performance is evaluated in three propagation environments by using different antenna types in Section V. Conclusions are given in Section VI.

2 System model

2.1 Mutual information

Consider the mutual information between $n_t \times 1$ channel input and $n_r \times 1$ noisy channel output, where channel input and the additive noise are assumed to be isotropic Gaussian complex variables. The expressions n_t and n_r denote the numbers of the transmitter and the receiver antennas, respectively. When the channel is known only at the receiver the mutual information can be expressed for the *i*th realization of the channel by [2]

$$I_{\mathbf{H}}^{(i)} = \log_2 \left| \mathbf{I} + \frac{\rho}{n_t} \mathbf{H}^{(i)} \mathbf{H}^{(i)H} \right|, \qquad i = 1 \ldots N_s, \tag{1}$$

where a channel matrix $\mathbf{H}^{(i)}$ is of size $n_r \times n_t$. The expression N_s stands for the number of channel realizations. Further, the expressions ρ, $|\bullet|$, and H denotes system SNR at the antenna reference point within the bandwidth of interest, determinant, and Hermitian transpose, respectively. In the case of unconstrained decoding complexity and fast fading channel conditions the Shannon capacity is given by $C = E[I_{\mathbf{H}}]$. However, a more practical measure for the performance of realistic MIMO systems that is valid with constrained decoding complexity is the outage mutual information defined by $\{t_p : \mathrm{Prob}(I_{\mathbf{H}}^{(i)} < t_p) = p\}$, where p denotes the outage probability [2].

2.2 Signal model

In this work the channel measurement system extended to capable of MIMO measurements [17] is used for the generation of measurement-based MIMO channel models. The parameter estimation procedure based on the work [19] provides information about the amplitudes, polarizations, angles of arrival, and delays of arriving multi-path (MP) components of the signal. The spherical antenna array utilized in parameter estimation is later described in Section IV, and more thoroughly in [19]. The experimental plane-wave based method (EPWBM), which accuracy is evaluated in [18], is used in combining the received signal with the radiation patterns of receiver antennas[1]. The analysis of this paper considers only narrowband systems. Hence, the estimated three-dimensional (3-D) signal distribution was summed in delay dimension producing a narrowband version of the received signal. The estimated MPs of the narrowband signal can be presented by using matrices of size ($n_r \times n_t$) for two orthogonal polarizations,

$$\mathbf{H}_x^{(i)(n)}(\theta_r, \phi_r) = \begin{bmatrix} h_{x,1}^{(i)(n)}(\theta_r, \phi_r) & \cdots & h_{x,n_t}^{(i)(n)}(\theta_r, \phi_r) \\ \vdots & \ddots & \vdots \\ h_{x,1}^{(i)(n)}(\theta_r, \phi_r) & \cdots & h_{x,n_t}^{(i)(n)}(\theta_r, \phi_r) \end{bmatrix}, \qquad n = 1 \ldots N, \tag{2}$$

[1] Measurement based antenna test bed (MEBAT) is the antenna evaluation method based on the EPWBM.

where the entries denote MPs that impinge to receiver antennas. The symbol x denotes either ϕ- or θ-polarized field component. Further, the expression N stands for the number of MPs, and symbols θ_r and ϕ_r denote the angles-of-arrival of MPs in elevation and azimuth, respectively. The radiation pattern matrix of receiver antenna system ($n_r \times n_t$) can be defined for two orthogonal polarizations by

$$\mathbf{G}_x^{(n)}(\theta_r, \phi_r) = \begin{bmatrix} g_{x,1}^{(n)}(\theta_r, \phi_r) & \cdots & g_{x,1}^{(n)}(\theta_r, \phi_r) \\ \vdots & \ddots & \vdots \\ g_{x,n_r}^{(n)}(\theta_r, \phi_r) & \cdots & g_{x,n_r}^{(n)}(\theta_r, \phi_r) \end{bmatrix}, \tag{3}$$

where the entries are the complex-valued samples of radiation patterns of AUTs for the direction of impinging MP. The effect of AUTs on the estimated signal distribution is defined by summing MPs of the signal

$$\mathbf{H}^{(i)} = \sum_{n=1}^{N} \left[\mathbf{M}_\phi^{(i)(n)}(\theta_r, \phi_r) \circ \mathbf{G}_\phi^{(n)}(\theta_r, \phi_r) + \mathbf{M}_\theta^{(i)(n)}(\theta_r, \phi_r) \circ \mathbf{G}_\theta^{(n)}(\theta_r, \phi_r) \right], \tag{4}$$

where '$\circ$' denotes elementwise (Schur-Hadamard) matrix product. While retaining the same realization, $\mathbf{M}^{(i)(n)}(\theta_r, \phi_r)$, the radiation patterns of AUTs, $\mathbf{G}^{(n)}(\theta_r, \phi_r)$, are implemented in post-processing to examine their effect on the channel, $\mathbf{H}^{(i)}$, and therefore on $I_{\mathbf{H}}^{(i)}$. The EPWBM enables efficient antenna evaluation with the minimal number of channel sounder measurements needed. It enables the rotation of radiation patterns of AUTs in azimuth and also in elevation to emulate different orientations of a communication device in real usage scenarios without performing separate measurements for the each orientation of an AUT.

3 Empirical evaluation methods of MIMO antenna systems

3.1 A general expression for MELG-adjusted mutual information

In the experimental analysis some reference power level has to be defined for comparable results in the evaluation of MIMO antenna systems. It has been verified that contradictory results occur by using different normalization methods [20], [21]. Depending on the power normalization scenario chosen the mutual information can be defined for the *i*th snapshot of the channel as

$$I_{\mathbf{H}}^{(i)} = \log_2 \left| \mathbf{I} + \frac{\rho}{n_t} \frac{\mathbf{H}^{(i)}\mathbf{H}^{(i)H}}{P_{norm}} \right|,$$

where

$$P_{norm} = \frac{1}{n_t n_r} \left\| \mathbf{H}_{sli}^{(i)} \right\|_F^2, \tag{5}$$

or, alternatively, as proposed in this paper by

$$P_{norm} = \frac{1}{n_t n_r} \left\| \mathbf{H}_{iso,sli}^{(i)} \right\|_F^2, \tag{6}$$

where $\left\| \bullet \right\|_F$ denotes the Frobenius norm. As will be shown in Section IV, no significant difference in the received powers between different antenna candidates were found when mutual information is defined based on (5); in this case the very same antennas that are under test are used in normalization. Alternatively, in expression (6), a common reference antenna system is used in the evaluation of AUTs. In that purpose a computational isotropic sensor defined by $E_{iso}(\theta,\phi) = \sqrt{E_\theta^2 + E_\phi^2} = 1$ gives the direction-independent reference. The symbols E_θ and E_ϕ represent θ and ϕ polarized signal components, respectively.

The effect of the slow fading is identified by taking a sliding mean over the power sequence of a reference antenna $\left\{ \left\| \mathbf{H}_{iso}^{(i)} \right\|_F^2 \right\}_{i=1}^{N_s}$ denoted by $\left\{ \left\| \mathbf{H}_{iso,sli}^{(i)} \right\|_F^2 \right\}_{i=1}^{N_s}$. This operation, when used in (6), mitigates the effect of slow fading due to obstacles in the propagation route, but, however, maintains the effect of signal fluctuation due to different orientations of AUTs. This is because the signal received by an isotropic sensor is independent of orientation. Based on the arguments presented the use of the expression (6) instead of (5) in the normalization is more objective approach in the antenna evaluation purpose.

3.2 Factorization of MELG-adjusted mutual information

After some manipulations of the expression (6) the mutual information (MI) can be expressed as

$$I_{\mathbf{H}}^{(i)} = \log_2 \left| \mathbf{I} + \rho n_r G_{ant}^{(i)} \frac{\mathbf{H}^{(i)}\mathbf{H}^{(i)H}}{\left\| \mathbf{H}^{(i)} \right\|_F^2} \right|, \tag{7}$$

where

$$G_{ant}^{(i)} = \frac{\left\|\mathbf{H}^{(i)}\right\|_F^2}{\left\|\mathbf{H}_{iso,sli}^{(i)}\right\|_F^2} \tag{8}$$

is the realization of instantaneous transferred signal power (TSP). It can be further factorized as

$$G_{ant}^{(i)} = \frac{P}{P_{iso}} \cdot \frac{\left\|\mathbf{H}^{(i)}\right\|_F^2}{P} \frac{P_{iso}}{\left\|\mathbf{H}_{iso,sli}^{(i)}\right\|_F^2} = G_{e,MIMO} \cdot G_{fad}^{(i)}, \tag{9}$$

where

$$G_{e,MIMO} = \frac{P}{P_{iso}} = \frac{\frac{1}{N_s}\sum_{i=1}^{N_s} P^{(i)}}{\frac{1}{N_s}\sum_{i=1}^{N_s} P_{iso}^{(i)}} = \frac{\frac{1}{N_s}\sum_{i=1}^{N_s}\left\|\mathbf{H}^{(i)}\right\|_F^2}{\frac{1}{N_s}\sum_{i=1}^{N_s}\left\|\mathbf{H}_{iso}^{(i)}\right\|_F^2}, \tag{10}$$

and

$$G_{fad}^{(i)} = \frac{\left\|\mathbf{H}^{(i)}\right\|_F^2}{P} \frac{P_{iso}}{\left\|\mathbf{H}_{iso,sli}^{(i)}\right\|_F^2}. \tag{11}$$

The empirical distribution of the transferred signal power (TSP), $\left\{G_{ant}^{(i)}\right\}_{i=1}^{N_s}$, is related to the radiation properties, orientations and locations of AUTs. The constant term $G_{e,MIMO}$, which is mean of the TSP and called a mean effective link gain (MELG), closely corresponds the definition of the mean effective gain (MEG) [6], [12] used in SISO antenna evaluation. Further, the variance of $\left\{G_{fad}^{(i)}\right\}_{i=1}^{N_s}$ characterizes the fluctuation of the TSP due to the channel and the antenna properties. The factorization based on (10) and (11) essentially defines the ability of MIMO antenna systems to transfer signal power between the transmitter and the receiver in comparison to an “isotropic” reference antenna system. It is assumed that the numbers and locations of “isotropic” sensors equals with the numbers and locations of AUTs. Generally, all non-idealities like dielectric and metallic losses as well as interaction between the antenna elements within array (mutual coupling) are included in the definition.

3.3 MELG-adjusted mutual information at high and low SNR range

At high SNR range, a lower bound for mutual information (1) can be derived by [22]

$$I_{\mathbf{H}}^{(i)} \approx K\log_2\left(G_{\sup}\right) + K\log_2\left(G_{fad}^{(i)}\right) + K\log_2\left(G_{mux}^{(i)}\right), \tag{12}$$

where $K = \min(n_r, n_t)$. In this paper, differing from the notation presented in [22], the MELG is included in the G_{sup}. In (12), the definition of the eigenvalue dispersion (ED) $G_{mux}^{(i)}$, which is a ratio of arithmetic ($m_a^{(i)} = \frac{1}{K}\sum_{k=1}^{K}\lambda_k^{(i)}$) and geometric ($m_g^{(i)} = \left(\prod_{k=1}^{K}\lambda_k^{(i)}\right)^{\frac{1}{K}}$) means of the eigenvalues of $\mathbf{H}^{(i)}\mathbf{H}^{(i)H}$, is used. The ED is a function of all the eigenvalues, which makes it an interesting figure of merit to characterize the spread of eigenvalues by using a single number. In the case of equal eigenvalues the ED goes to unity ($G_{mux}^{(i)} = 1$), whereas in the case of at least one zero eigenvalue the ED goes to zero ($G_{mux}^{(i)} = 0$). Basically the expression $K\log_2\left(G_{mux}^{(i)}\right)$ defines the loss in mutual information from the ideal (supremum) case. The ED is not the new concept; it is called an ellipticity statistic in [23], a minimum description length (MDL) in [24], and a sphericity test in [25]. However, in the context of MIMO system evaluation it is introduced first time in [22].

At low SNR range, a lower bound of mutual information is stated e.g. in [5]. By introducing the MELG it can be re-expressed as

$$I_{\mathbf{H}}^{(i)} \approx \log_2\left[1 + \rho \cdot n_r \cdot \frac{\left\|\mathbf{H}^{(i)}\right\|_F^2}{\left\|\mathbf{H}_{iso,sli}^{(i)}\right\|_F^2}\right] = \log_2\left[1 + \rho \cdot n_r \cdot G_{e,MIMO} \cdot G_{fad}^{(i)}\right], \tag{13}$$

which shows no effect of the ED ($G_{mux}^{(i)}$). Thus, in theoretical point of view the effect of the ED is negligible at low SNR range. However, it is shown later with realistic radio channels that the effect of the TSP dominates also at relatively high SNR range.

3.4 Significance of factorization

The distributions (e.g. cdf) of $\left\{G_{ant}^{(i)}\right\}_{i=1}^{N_s}$ and $\left\{G_{mux}^{(i)}\right\}_{i=1}^{N_s}$ essentially define the properties of a MIMO system. The factorization delivers information not only from the parallel channels but also from the signal power transferring properties of the antenna systems. Some evident observations can be given based on the factorization: The MELG of the antenna system directly modifies system SNR (ρ). Further, by increasing the number of receiving antenna elements in the array the relative effect of the MELG degreases, meaning that the properties of a specific antenna element become less significant in larger MIMO systems.

4 Antenna evaluation system

4.1 Measurement system

4.1.1 Measurement antennas

Measurements were done with the wideband channel sounder developed for 2 GHz range [19], [17]. The investigations using the measured channels and four 2×2 MIMO antenna systems were carried out to validate the effect of the antennas on the performance of MIMO systems. The measurement antenna arrays, which are a linear in indoors and a zigzag in outdoors (8 elements selected from 16 ones corresponding 16 channels) at the Tx and a spherical (32 elements, 64 channels) at the Rx, were equipped with the similar dual–polarized patch antennas [19]. The patch antennas used have directivity of 7.8 dBi and 6 dB beam width of 90° and 100° for the vertically and horizontally polarized feeds, respectively [19]. The measurement antenna arrays are presented in Fig.1.

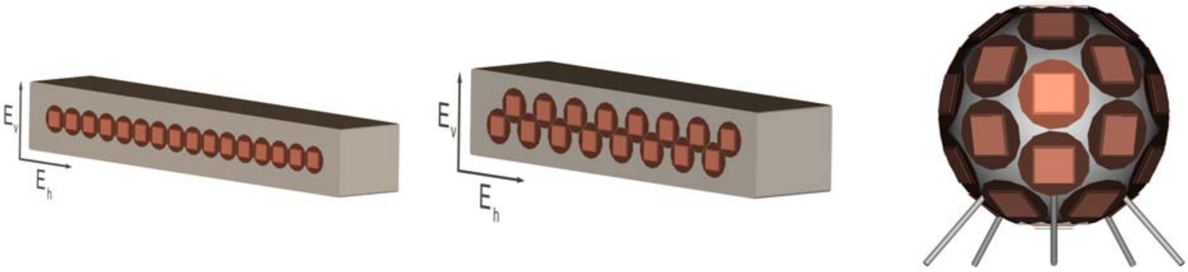

a) b) c)

Figure 1. Antenna arrays used in measurements: a) linear (Tx), b) zigzag (Tx), c) spherical (Rx).

4.1.2 Measurement routes

Measurement routes: Microcell (LOS) and small macrocell (NLOS) routes were measured in Helsinki city center. The transmitter antenna was located on the roof of a Kaisa shopping center in the small macrocell (NLOS) measurement, and elevated at a height of 4 m by using a crane in the microcell (LOS) measurement. Indoor route was measured in the modern computer science building of TKK, where the transmitter antenna was placed at a height of 3.8 m. The measurement routes and the fixed station (FS) locations are presented in Fig. 2. The channel sounder is capable of measuring a full wideband 16×64 channel matrix in 8.7 ms; during that time the measurement trolley moves only 4.3 mm (the speed of the trolley was about 0.5 m/s). The waiting time between two consecutive measurements is 63 ms. Hence, a sample from the dynamic channel is taken in every 72 ms.

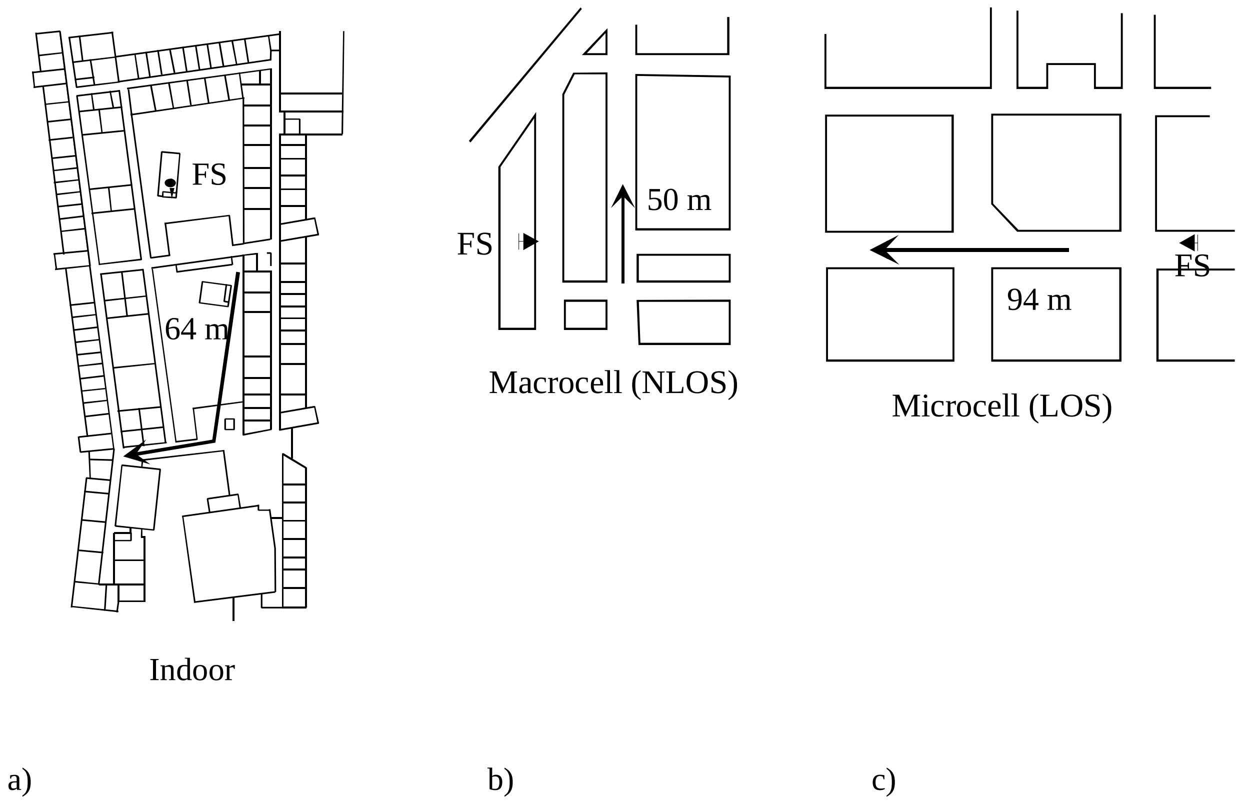

Figure 2. Measurement routes used in the analysis: a) indoor, b) small macrocell (NLOS), c) microcell (LOS). Orientations of the transmitter antennas (FS) and the measurement routes are presented using the arrows.

4.2 Accuracy of measurement system

The possible error sources of the MIMO measurement system are thermal and phase noise, quantization noise as well as spurious signals in frequency synthesizers. The effect of phase noise error is considered in [26] and the effect of thermal noise error is studied in [27] and [28]. Generally, the error increases when the measurement SNR decreases and the system SNR as well as the number of antennas increases. The measurement SNR is defined for the measured impulse responses before multidimensional estimation of the channel. The thermal noise error of the 2 GHz measurement system used was estimated to be below 1 bit/s/Hz with the measurement SNR of 22 dB[2] and the system SNR of 10 dB for a 4×8 MIMO system in [13]. The similar measurement system for 5 GHz range was evaluated in [29] where the error of the mutual information was estimated to be less than 2 bit/s/Hz for a 4×4 MIMO system in rank one case with the system SNR of 30 dB. Based on the analysis presented in [27] overestimation of the capacity for a 2×2 MIMO system in rank one channel (the worst scenario) with the system SNR of 30 dB is 1.7 bit/s/Hz. However, the results in [30] imply that degenerate channels (rank one) are uncommon in the real signal propagation environments. Hence, the error of the mutual information for the 2×2 MIMO system used is approximated to be much less than 1.7 bit/s/Hz with the system SNR of 30 dB.

[2] This represents the most pessimistic scenario in error point of view, typically measurement SNR is about 30 dB.

4.3 Investigated antenna types

2×2 MIMO antenna systems with considerably different radiation and polarization properties were purposefully selected for revealing possible critical phenomena from the results. Four antenna scenarios as well as a reference scenario with isotropic antennas were considered:

- Two vertically polarized feeds from the patch antennas at the Tx (Fig. 1) and two vertically polarized dipole antennas at the Rx (*ver_dip*).
- Vertically and horizontally polarized feeds from the patch antennas at the Tx and vertically and horizontally polarized dipole antennas at the Rx (*cro_dip*).
- Two vertically polarized feeds from the patch antennas at the Tx and two vertically polarized directive antennas at the Rx (*ver_dir*).
- Vertically and horizontally polarized feeds from the patch antennas at the Tx and vertically and horizontally polarized directive antennas at the Rx (*cro_dir*).
- Two vertically polarized feeds from the patch antennas at the Tx and two isotropic sensors at the Rx (*iso*).

The radiation pattern function of the ideal directive antenna element is of the form $[\sin(\theta)\cos(\phi)]^n$ possessing the directivity of 7.8 dBi and the 3 dB beamwidth of 90°, where $\theta \in [0^\circ, 180^\circ]$ and $\phi \in [-90^\circ, 90^\circ]$ denotes the elevation and azimuth angle, respectively. Further, the dipole antennas possess the ideal directivity of 2.1 dBi. The spacing of the antenna elements within the antenna systems was 0.5λ at the both ends of the link in all the other cases but indoors where the spacing of the Tx elements was 0.7 λ (see Fig. 1a). The sketch of the radiation patterns and the polarizations of the investigated antennas are depicted in Figs. 3a and b, respectively. The effect of antenna orientation was simulated rotating the radiation patterns of the Rx arrays with 30° steps in azimuth. The array orientation coordinates relative to the street and the direction of motion of the measurement trolley in the measurements are presented in Fig. 4. After concatenation of the results of each rotation of the Rx antenna array the number of snapshots (N_s) in the cases of the macrocell (NLOS), the microcell (LOS), and the indoor were 16104, 30000, and 20604, respectively[3]. After concatenation, slow fading was removed from the signal by using a sliding window of about 20 λ.

a) b)

Figure 3. a) Sketch of the radiation patterns used in the analysis (from above). b) Sketch of the polarizations used in the analysis (from side).

[3] The number of snapshots before rotation in the cases of macrocell, microcell (LOS) and indoor were 1342, 2500, and 1717, respectively. About 4 samples per wavelength were taken which corresponds the route lengths of 47m, 87m and 60m, respectively.

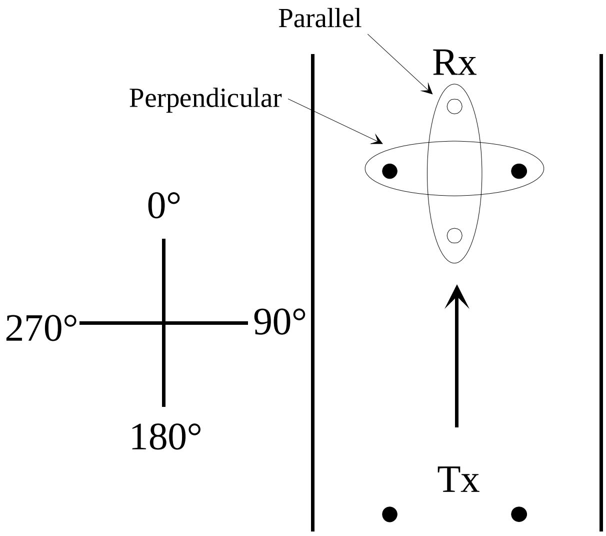

Figure 4. Rx antenna array orientations relative to Tx antenna array orientation as arranged in the microcell (LOS) environment. Patch antenna elements of the Tx antenna array are pointing to the direction of 0°.

5 Empirical MIMO antenna evaluation

In the evaluation of the antennas the sequences of $\left\{I_{\mathbf{H}}^{(i)}\right\}_{i=1}^{N_s}$, $\left\{G_{mux}^{(i)}\right\}_{i=1}^{N_s}$ and $\left\{G_{ant}^{(i)}\right\}_{i=1}^{N_s}$ for the mutual information (MI), for the eigenvalue dispersion (ED), and for the transferred signal power (TSP) are analyzed, respectively. The outage probability is defined by using the well-known expression $\left\{t_p : \mathrm{Prob}\left(X < t_p\right) = p\right\}$, where $X = \left\{I_{\mathbf{H}}^{(i)}\right\}_{i=1}^{N_s}; \left\{G_{mux}^{(i)}\right\}_{i=1}^{N_s}; \left\{G_{ant}^{(i)}\right\}_{i=1}^{N_s}$. Either the whole cumulative distribution function (cdf) is visually inspected, or some probability level (p) of it is chosen. The analysis of $\left\{I_{\mathbf{H}}^{(i)}\right\}_{i=1}^{N_s}$ at p = 1% and 50% as a function of SNR (ρ) and cdfs of $\left\{G_{mux}^{(i)}\right\}_{i=1}^{N_s}$ and $\left\{G_{ant}^{(i)}\right\}_{i=1}^{N_s}$ are presented. Depending on the analysis, whether the results as a function of antenna orientation or the concatenated results of the 12 antenna orientations are presented. The most significant results are given in this section. All the results considering the three different environments and the four Rx antenna systems are given in Appendix. The results of identically and independently distributed (iid) Rayleigh channel are also shown in Appendix.

5.1 Eigenvalue dispersion (ED)

5.1.1 Directivity

The effect of radiation pattern on the results of the eigenvalue dispersion (ED) when using the vertically polarized antennas was studied first. It was found that the use of the directive antennas (*ver_dir*) results in the smaller ED than the use of the dipoles (*ver_dip*), especially in the microcell (LOS) scenario (see Fig. 5a). For further investigation the results of the ED were studied as a function of antenna orientation at p = 50% in Fig. 5b. The Rx array, where the directive elements were pointing to equal directions, was rotated gradually in azimuth to the 12 different orientations[4]. Aligning the Rx antenna array perpendicular to the street according to black dots in Fig. 4 (main lobes pointing to the direction of 180°) shows the maximum ED. On the other hand, the minimum ED was achieved when the array was rotated 180° in azimuth to the direction of 0° (main lobes pointing to the direction of 0°). In this unfavourable orientation the array faces more scattering due to the reflections of the signal from the surrounding objects. Hence, it receives two channels with a rather small power imbalance resulting the small ED, that is, a value close to unity. On the other hand, when the main lobes of the antennas on the Tx and the Rx arrays are pointing against the each other only one dominant eigenvalue exists, which increases the ED (value much smaller than one). Hence, it is verified that the ED of the *ver_dir* depends strongly on the orientation of the array. The variation of the ED was smaller in the case of the dipole antennas. The minimum ED was achieved when the array is perpendicular to the street because in that position the aperture of the array is maximized relative to arriving signal. Similar result was found for a 6×6 MIMO system in [31]. It was also found that the variance of the ED is smaller in comparison to the directive antennas. Hence, based on this study, the directive and the omnidirectional Rx antennas show significantly different behaviour in the ED due to the different radiation properties of the antennas. In the other more scatter-rich environments the results of the ED differ less from each other for the investigated antenna scenarios as can be seen from the results in Appendix.

[4] The coordinate system used is presented in Fig 4.

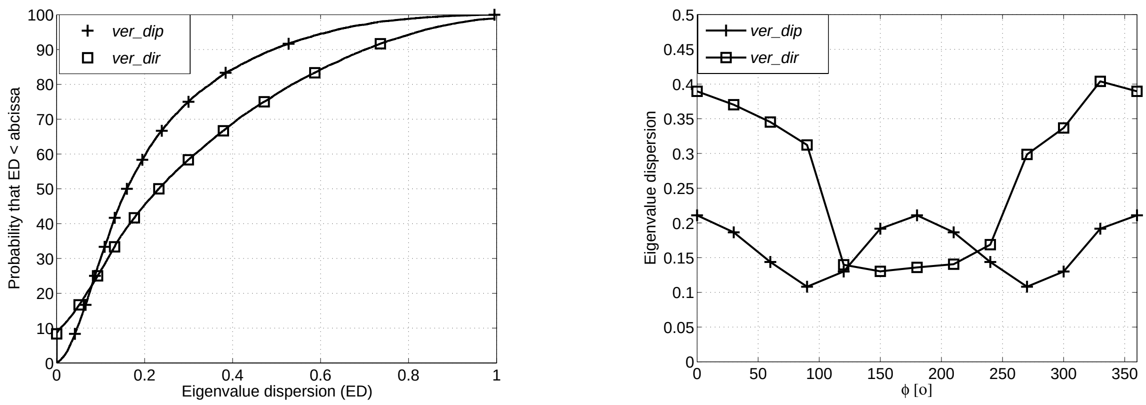

a) b)

Figure 5. Comparison of eigenvalue dispersion (ED) results with the directive and the omnidirectional antennas in the microcell (LOS) scenario. a) Cdfs of ED. b) ED as a function of antenna orientation at p = 50%.

5.1.2 Polarization

With the 2×2 MIMO system, the scenarios of using one or two polarizations in the ideal LOS conditions with no scattering (infinite Rice factor), has been discussed in [32]. It was shown in [32] that the channel degenerates when using only one polarization, the case of where only a single eigenvalue exists ($G_{mux}^{(i)} = 0$). On the other hand, when using two polarizations instead of one two identical eigenvalues exist ($G_{mux}^{(i)} = 1$). In this paper, the same type of scenario is investigated in the realistic environments using the vertically (*ver_dip*) and the orthogonally (*cro_dip*) polarized dipole antennas including also the rotation of the Rx array. The ED results of two signal propagation environments, the indoor and the microcell (LOS), were considered in Fig. 6a. As expected, the use of the two orthogonal polarizations produces the smaller ED compared to the use of the single polarization, also verified in [20]. Further, due to increased scattering the ED of the *ver_dip* is smaller in the indoor than in the microcell (LOS) scenario.

Generally the rich scattering of multi-paths causes crosstalk between the polarizations. However, based on this study, there occur no significant changes in the results of the ED when using the orthogonally polarized dipoles (*cro_dip*) in the considered environments (see Fig. 6a). Thus, the ED of the *cro_dip* is more robust for the environmental variations than the ED of the *ver_dip*. Further, the result depends on the considered probability level; the curves of the two environments cross at the level of 33%. Clearly, the use of the two orthogonal polarizations makes the system more insensitive for the environmental variations. On the other hand, the ED of the *cro_dip* depends very strongly on the orientation of the antenna array, especially in the microcell (LOS) scenario. The minimum ED, which is almost in the same level as with the *ver_dip*, was found when the *cro_dip* is parallel with the street. This result is presented for p = 50% in Fig. 6b. All the results of the ED are presented in Appendix.

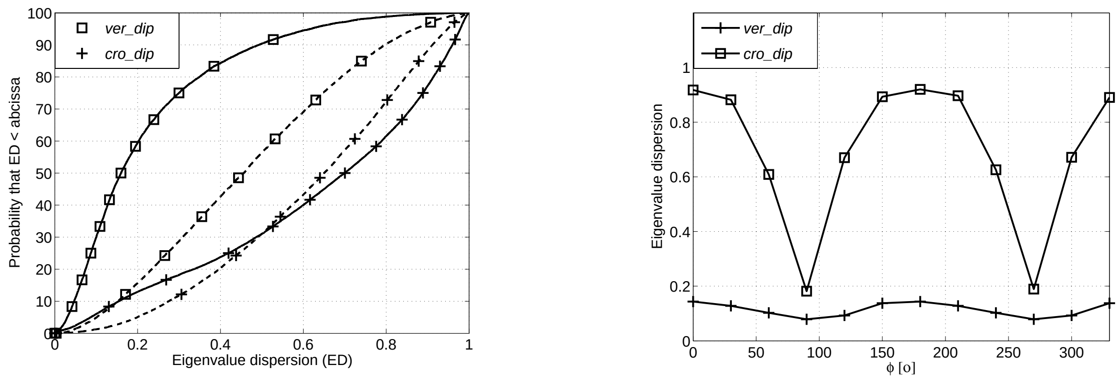

a) b)

Figure. 6. a) Cdfs of eigenvalue dispersion (ED) for vertically (*ver_dip*) and orthogonally (*cro_dip*) polarized dipoles presented in the microcell (LOS) (solid line) and indoor (dotted line) scenarios. b) ED presented at p = 50% as a function of Rx antenna orientation in the microcell (LOS) scenario.

5.2 Transferred signal power (TSP) of the antenna systems

5.2.1 Normalization

The results of using the two different normalizations are considered demonstrating the significant differences in the mean and the variance of the transferred signal power (TSP) between the power normalization methods. The results of using the expressions (5) and (6) are presented in Figs. 7a and b, respectively, considering all the Rx antenna systems in the microcell (LOS) scenario. The normalization (6) shows clear differences in the variance and the mean of the TSP between the considered antennas, which, however, is not the case when using the normalization (5). Especially significant differences were noticed with the directive antennas. The differences between the results are smaller in the other more scatter-rich environments where the antenna systems are less orientation sensitive as can be seen in Appendix.

5.2.2 Directivity

The differences in the TSP between the antenna systems can be significant depending on the considered outage probability level. The variance of the TSP is higher with the directive antennas, which makes them more sensitive to an antenna orientation (and more unreliable) than the omnidirectional ones. The highest variance of the TSP was found in the microcell due to the street canyon effect – a receiver antenna system can be badly oriented in proportion to the arriving signal distribution (see Fig. 7b). The maximum difference of the power levels when comparing the results of the *cro_dir* and the *ver_dip* is about 23 dB at p = 10%! The result of using the isotropic sensors (*iso*) at the Rx is also presented. It represents the scenario independent of the radiation pattern, and hence, a yardstick for the TSP of the AUTs. In the more scatter–rich environments the results of the TSP approaches to the each other (see Appendix).

5.2.3 Polarization

Finally, the differences of the TSP when using one or alternatively two orthogonal polarizations in the antenna systems are compared. The use of two polarizations decreases the TSP in comparison to the use of single polarization only. This is demonstrated by the means of the

MELG, the results of which are presented for the considered antenna systems in Fig. 8. The difference of the TSP is up to 6 dB with the considered antennas. The results approach to each other in the other environments, which can be seen in Appendix. This is because for single polarized antennas some of the signal power is lost in highly scatter–rich environment due to polarization mismatch. On the other hand, there is not the same problem with two orthogonal polarizations if an antenna array is beneficially aligned. This makes the systems with two orthogonal polarizations more robust for the environmental variations but also more orientation sensitive than the use of single polarization – the very same result that was achieved with the results of the ED.

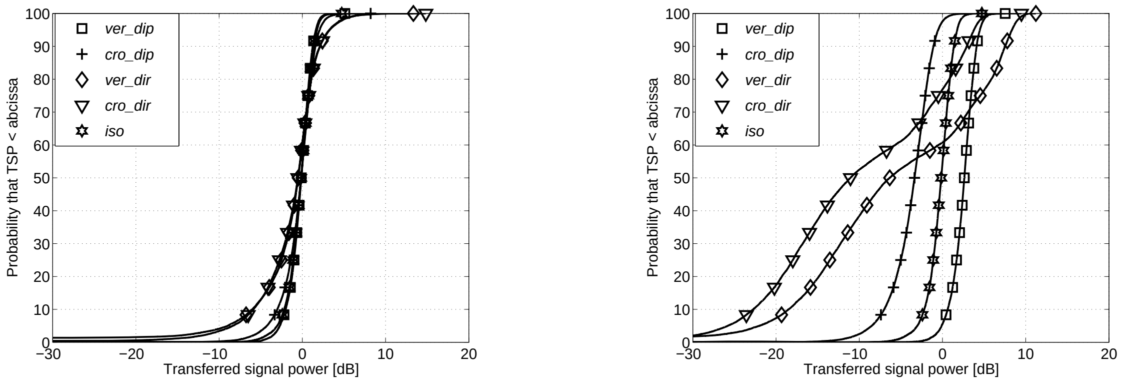

a) b)

Figure. 7. Effect of normalization on transferred signal power (TSP). a) Normalization scenario based on (5). b) Normalization scenario based on (6).

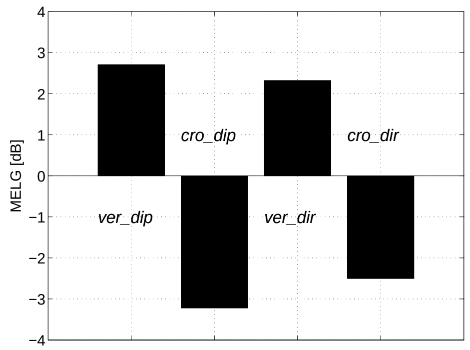

Figure 8. Results of mean effective link gain (MELG) presented for the considered antenna systems in the microcell (LOS) scenario.

5.3 Effect of ED and TSP on mutual information (MI)

Based on the expressions (7) and (12), the mutual information (MI) generally depends both on the eigenvalue dispersion (ED) and the transferred signal power (TSP). However, as was verified earlier, the value of those parameters depends on the antennas used, the array orientation and also the signal propagation environment. Fig. 9 presents the results of the outage MI for all the considered antennas at the probability levels of 1% and 50% as a function of ρ in the microcell (LOS) scenario. Evidently, the performance of the antenna systems is related also to the level of ρ and p. E.g. due to the better TSP of the *ver_dip* it performs better than the *cro_dip* at p = 1%, but the results approach to the each other at p = 50% because the smaller ED of the latter case. Generally, the variation of the MI results between the used antennas is larger at low than at high probability levels. This is mainly due to the higher differences of the TSP between the antennas. The antennas with the omnidirectional radiation patterns perform better than the antennas with the directive radiation patterns; 1% outage MI is especially low with the arrays of the directive antennas in the microcell (LOS) scenario. However, the MI results of the different antenna scenarios approach to the each other when the environment becomes more scatter–rich, that is, the performances of the antennas almost equals at p = 50% (see Appendix). The results also show no significant degradation of the MI in comparison to the iid Rayleigh channel.

Evidently the TSP dictates, in general, the performance of the small MIMO systems. Based on that the low SNR approximation of the MI (13) would evidently rank the antennas correctly even at ρ = 30 dB and p = 1% in the considered cases. However, the effect of the low ED becomes more significant with the *cro_dip* at p = 50% as can be seen in Fig. 9b. The differences of the TSP when using more realistic antenna prototypes can be even more significant due to the realistic efficiencies (in this study the efficiencies were assumed to be ideal). Further studies should also be carried out for the larger MIMO systems. In those cases the effect of the ED begins to dominate and the high SNR approximation of the MI (12) will probably be valid.

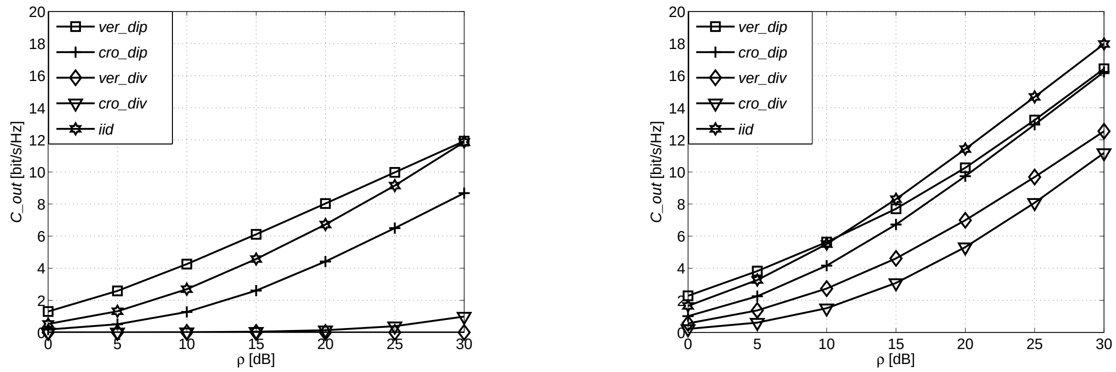

a) b)

Figure. 9. Outage mutual information (MI) presented as a function of system signal-to-noise-ratio ρ in the microcell (LOS) scenario. a) Probability level p = 1%. b) Probability level p = 50%.

6 Conclusion

In this paper, a new approach that takes into account both the ability to utilize parallel spatial channels and the signal power transferring properties of the antennas is proposed to the comprehensive MIMO antenna system performance study. The factorization consists of two parameters: the transferred signal power (TSP), and the eigenvalue dispersion (ED). The TSP can be further factorized into the mean effective link gain (MELG), and the SNR fading. A common reference power level is essential in the factorization for the reliable identification of the performance differences between different antenna systems.

The effect of the antennas on the MIMO performance is considered by using the four ideal antenna types in the three measured channels. An antenna array orientation as well as the radiation properties of antenna elements, that is, the shapes of radiation patterns and polarizations, influences the realized capacity of a MIMO system. Further, the performance of MIMO antenna system is related to the signal-to-noise-ratio as well as to the required reliability of the system. The following main observations are made from the results:

- Proper power normalization is vital for the fair comparison of the antennas with directive patterns because the antenna performance depends heavily on the antenna orientation. For the same reason, the rotation of radiation patterns of the antennas is essential for the unbiased evaluation of the TSP properties especially at low outage probability levels.
- The ability to transfer signal power (TSP) between the Tx and Rx dominates the mutual information even at the relatively high signal-to-noise-ratios in the case of small MIMO systems. In the most of the cases the performance of MIMO system can be predicted directly based on the TSP.
- The performance differences between the antennas are larger at low than at high outage probability levels due to the different radiation properties of the antennas.
- When considering the ED, the TSP and thus the MI, the antenna systems utilizing two orthogonal polarizations are more robust to the environmental variations but less robust to the different antenna orientations in comparison to the single polarization antenna systems.
- The highest differences in the outage MI results between the antennas are found in the microcell (LOS) scenario where the signals are clusterized due to the street canyon effect.
- The best antenna performance is achieved with the vertically polarized dipole antennas (*ver_dip*) at low outage probability level (p=1 %).

Appendix

Four 2×2 MIMO antenna systems are analyzed in three considered environments. Results of small macrocell (NLOS), microcell (LOS) and indoor environments are presented in Figs. 10, 11 and 12, respectively.

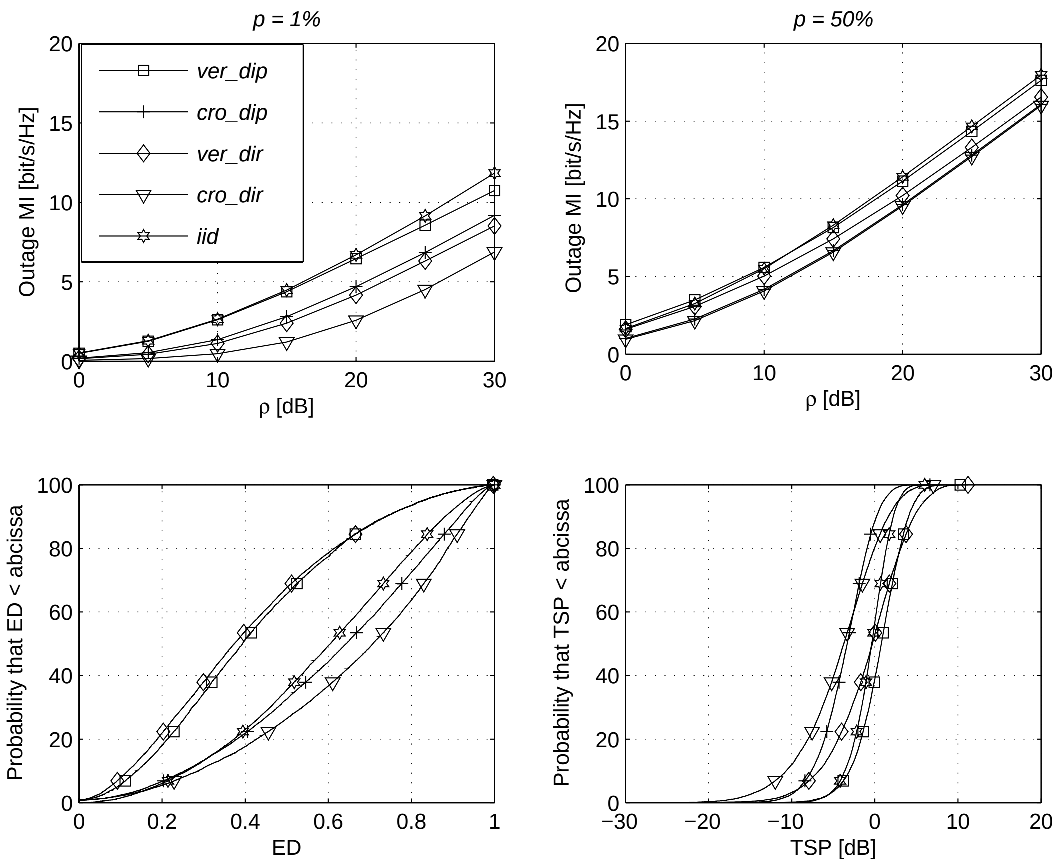

Figure 10. Four 2×2 MIMO systems are analyzed in the small macrocell (NLOS) case. Results of outage MI, ED and TSP are considered at different subplots. Analysis of outage MI is presented in the capacity outage probability levels (p) of 1% and 50% as a function of ρ in the upper figures. The cdfs of ED and TSP are presented in the lower figures.

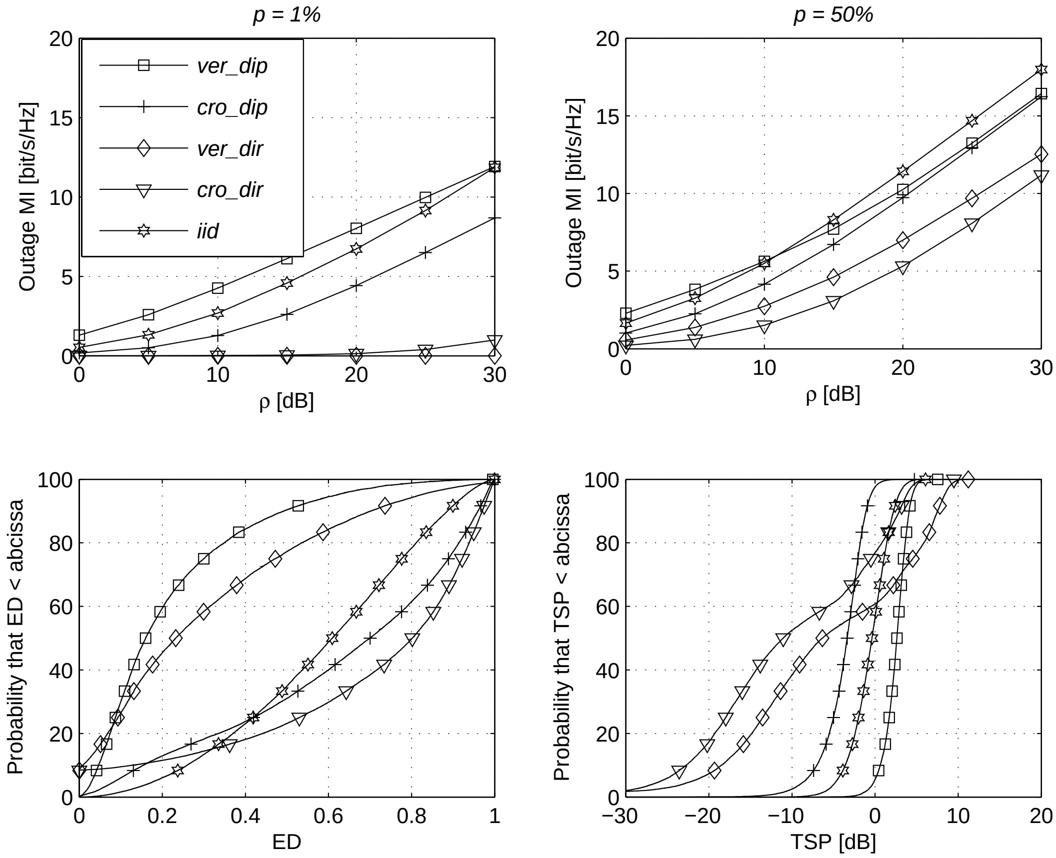

Figure 11. Four 2×2 MIMO systems are analyzed in the microcell (LOS) case. Results of outage MI, ED and TSP are considered at different subplots. Analysis of outage MI is presented in the capacity outage probability levels (p) of 1% and 50% as a function of ρ in the upper figures. The cdfs of ED and TSP are presented in the lower figures.

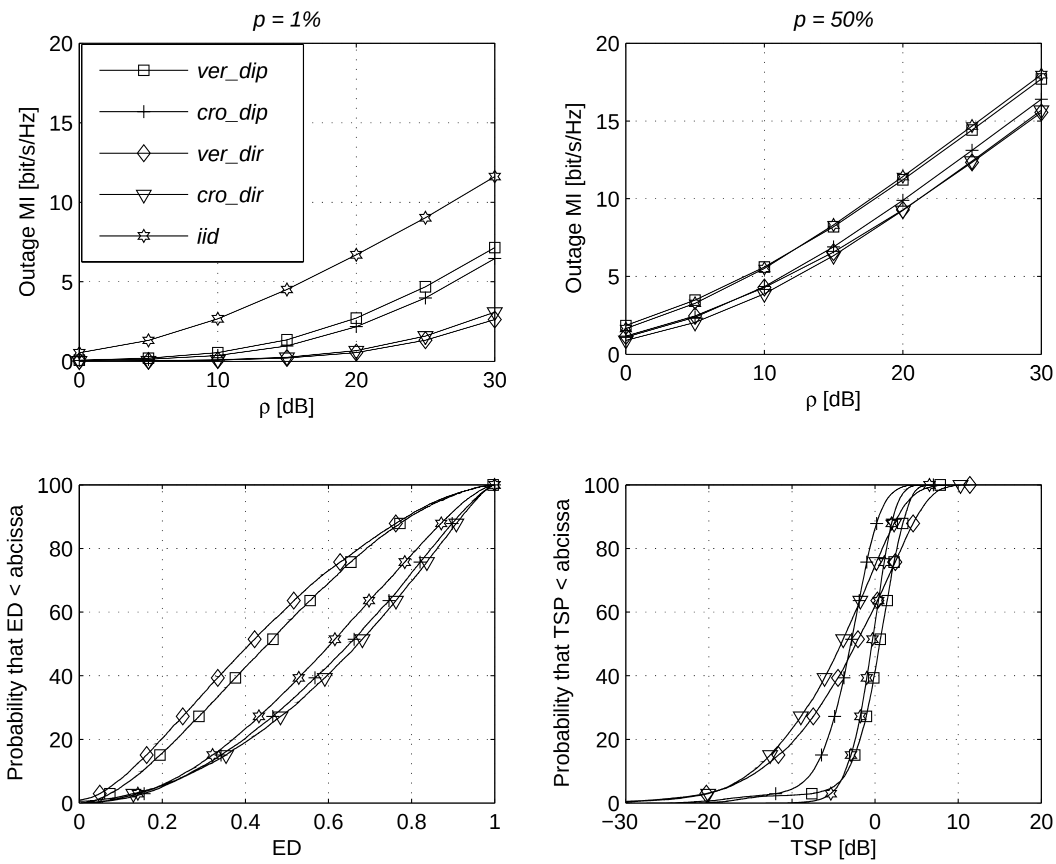

Figure 12. Four 2×2 MIMO systems are analyzed in the indoor case. Results of outage MI, ED and TSP are considered at different subplots. Analysis of outage MI is presented in the capacity outage probability levels (*p*) of 1% and 50% as a function of ρ in the upper figures. The cdfs of ED and TSP are presented in the lower figures.

Acknowledgments

We would like to thank Nokia foundation, Finnish cultural foundation, and Academy of Finland for the financial support of this work.

References

[1] G. J. Foschini, M. J. Gans, ”On limits of wireless communications in a fading environment when using multiple antennas,” *Wireless Personal Communications*, vol. 6, no. 6, pp. 311–335, Mar. 1998.

[2] I.E. Telatar, “Capacity of multi-antenna Gaussian channels”, *European Transactions on Telecommunications*, vol. 10**,** no. 6, pp. 585–595, Nov./Dec.1999.

[3] L. Zheng and D.N.C. Tse, “Diversity and multiplexing: a fundamental tradeoff in multiple-antenna channels”, *IEEE Trans. Inform. Theory*, vol. 49, no 5, pp. 1073–1096, May 2003.

[4] W. Weichselberger, “Spatial Structure of Multiple Antenna Radio Channels: A Signal Processing Viewpoint”, *PhD thesis*, Vienna University of Technology, 2003.

[5] Ö. Oyman, R. U. Nabar, H. Bölcskei, and A. J. Paulraj, “Characterizing the statistical properties of mutual information in MIMO channels”, *IEEE Trans. Signal Processing*, vol. 51, no. 11, pp. 2784–2795, Nov. 2003.

[6] J. B. Andersen and F. Hansen, “Antennas for VHF/UHF personal radio: A theoretical and experimental study of characteristics and performance,” *IEEE Trans. Veh. Technol.,* vol. VT-26, no. 4, pp. 349–357, Nov. 1977.

[7] K. Sulonen, P. Vainikainen, “Performance of mobile phone antennas including effect of environment using two methods,” *IEEE Trans. Instrum. Meas.,* vol. 52, no. 6, pp.1859–1864, Dec. 2003.

[8] C.B. Dietrich, K. Dietze, J.R. Nealy, and W.L. Stutzman, “Spatial, polarization, and pattern diversity for wireless handheld terminals”, *IEEE Trans. Antennas Propagat.*, vol. 49, no. 9, pp. 1271–1281, Sep. 2001.

[9] J. Villanen, P. Suvikunnas, K. Sulonen, C. Icheln, J. Ollikainen and P. Vainikainen, ”Advances in diversity performance analysis of mobile terminal antennas,” in *Proc. 2004 International Symposium on Antennas and Propagation*, CD-Rom (ISBN 4-88552-208-0), paper 3A3-3.pdf, 2004, pp. 649–652.

[10] B.M. Green, M.A. Jensen, “Diversity performance of dual-antenna handsets near operator tissue”, *IEEE Trans. Antennas Propagat.*, vol. 48, no. 7, pp. 1017–1024, Jul. 2000.

[11] P.S. Kildal and K. Rosengren, “Electromagnetic analysis of effective and apparent diversity gain of two parallel dipoles”, *IEEE Antennas and Wireless Propagation Letters*, vol. 2, no. 1 , pp. 9–13, Dec. 2003.

[12] T. Taga, “Analysis for mean effective gain of mobile antennas in land mobile radio environments,” *IEEE Trans. Veh. Technol.*, vol. 39, no. 2, pp. 117–131, May 1990.

[13] K. Sulonen, P. Suvikunnas, L. Vuokko, J. Kivinen, P. Vainikainen, “Comparison of MIMO antenna configurations in picocell and microcell environments,” *IEEE J. Select. Areas Commun*, vol. 21, no. 5, pp. 703–712, Jun. 2003.

[14] J. P. Kermoal, P. E. Mogensen, S. H. Jensen, J. B. Andersen, F. Fredriksen, T. B. Sorensen, K. I. Pedersen, “Experimental investigation of multipath richness for multi-element transmit and receive antenna arrays,” in *Proc. IEEE 51th Vehicular Technology Conf. (spring)*, vol. 3, 2000, pp. 2004–2008.

[15] C. C. Martin, J. H. Winters, N. R Sollenberger, “Multiple-Input – Multiple-Output (MIMO) radio channel measurements,” in *Proc. IEEE 52th Vehicular Technology Conf. (fall).*, vol.2, 2000, pp. 774–779.

[16] D. Chizhik, J. Ling, P. W. Wolniansky, R. A. Valenzuela, N. Costa, and K. Huber, ”Multiple-Input – Multiple-Output measurements and modeling in Manhattan,” *IEEE J. Select. Areas Commun.*, vol. 21, no. 3, pp. 703–712, Apr. 2003.

[17] J. Kivinen, P. Suvikunnas, D. Perez, C. Herrero, K. Kalliola, P. Vainikainen, “Characterization system for MIMO channels,” in *Proc. 4th Int. Symp. Wireless Personal Multimedia Communications*, 2001, pp. 159–162.

[18] P. Suvikunnas, K. Sulonen, J. Villanen, C. Icheln, P. Vainikainen, “Evaluation of performance of multi-antenna terminals using two approaches,” in *Proc. IEEE 21th Instrum. and Meas. Technol. Conf.*, vol. 2, 2004, pp. 1091–1096.

[19] K. Kalliola, H. Laitinen, L. Vaskelainen, and P. Vainikainen, ”Real-time 3-D spatial-temporal dual-polarized measurement of wideband radio channel at mobile channel,” *IEEE Trans. Instrum. Meas.*, vol. 49, no. 2, pp. 439–446, Apr. 2000.

[20] P. Suvikunnas, J. Salo, J. Kivinen, P. Vainikainen, “Comparison of MIMO antennas: performance measures and evaluation results of two 2x2 antenna configurations,” *Nordic Radio Symposium 2004*, CD-Rom (ISBN 951-42-7419-9), paper WEDAM7_1.pdf, 2004.

[21] J. Salo, B. Badic, P. Suvikunnas, H. Weinrichter, M. Rupp, and P. Vainikainen, “Influence of antenna configurations on performance of STBC in urban microcells,” *IEE Electronics Letters*, vol. 41, no. 21, pp. 1157–1158, Oct. 2005.

[22] J. Salo, P. Suvikunnas, and P. Vainikainen, “Some results on MIMO mutual information: the high SNR case”, *Globecom’04*, vol. 2, 2004, pp. 943-947.

[23] R. Muirhead, *Aspects of multivariate statistical theory*, John Wiley and Sons, Inc., 1982.

[24] M. Wax, I. Ziskind, “Detection of the number of coherent signals by the MDL pronciple,” IEEE Trans. Acoustics, Speech, and Signal Processing, vol. 37, no. 8, pp. 1190–1196, Aug. 1989.

[25] D. Williams, D. Johnson, “Using the spericity test for source detection with narrowband passive arrays,” IEEE Trans. Acoustics, Speech, and Signal Processing, vol. 38, no. 11, pp. 2008–2014, Nov. 1990.

[26] D. S. Baum, and H. Bölcskei, “Inpact of phase noise on MIMO channel measurement accuracy,” in *Proc. IEEE 60th Veh. Technol. Conf. (fall)*, vol. 3, 2004, pp. 1614–1618.

[27] N. Amitay, M. J. Gans, H. Xu, and R. A. Valenzuela, “Effects of thermal noise on accuracy of measured BLAST capacities,” *IEE Electronics Letters*, vol. 37, no. 9, pp. 591–592, Apr. 2001.

[28] M. J. Gans, N. Amitay, Y. S. Yeh, H. Xu, T. C. Damen, R. A. Valenzuela, T. Sizer, R. Storz, D. Taylor, W. M. MacDonald, C. Tran, A. Adamiecki, “Outdoor BLAST measurement system at 2.44 GHz: Calibration and initial results,” *IEEE J. Select. Areas Commun.*, vol. 20, no. 3, pp. 570–583, Apr. 2002.

[29] V.-M. Kolmonen, J. Kivinen, L. Vuokko, and P. Vainikainen, ”5.3 GHz MIMO radio channel sounder”, in *Proc. 22th IEEE Instrum. and Meas. Technol. Conf.*, vol. 3, 2005, pp. 1883–1888.

[30] P. Almers, F. Tufvesson, and A. F. Molich, “Measurement of keyhole effect in a wireless multiple-input multiple-output (MIMO) channel,” *IEEE Commun. Lett.*, vol. 7, no. 8, pp. 373 – 375, Aug. 2003.

[31] P. Almers, F. Tufvesson, P. Karlsson, and A. Molisch, “The effect of horizontal array orientation on MIMO channel capacity,” in *Proc. IEEE 57th Veh. Technol. Conf. (Spring)*, vol. 1, 2003, pp. 34–38.

[32] A. Paulraj, R. Nabar, and D. Gore, *Introduction to Space-Time Wireless Communications*, Cambridge University Press, 2003, 277 p.

S 265 Sulonen, K.
Evaluation of performance of mobile terminal antennas, June 2004

S 266 Ollikainen, J.
Design and implementation techniques of wideband mobile communications antennas, November 2004

S 267 Hienonen, S.
Studies on microwave antennas: passive intermodulation distortion in antenna structures and design of microstrip antenna elements, March 2005

S 268 Räisänen, A.V., Lindberg, S.
TKK Radio Laboratory research and education 2004, March 2005

S 269 Möttönen, V.S.
Receiver front-end circuits and components for millimetre and submillimetre wavelengths, April 2005

S 270 Chicherin, D., Tretyakov, S.
Third annual SMARAD centre of excellence research seminar, April 2005

S 271 Räisänen, A.V., Jääskeläinen, A.
SMARAD Smart and Novel Radios Research Unit Activity Report 2002-2004, June 2005

S 272 Kivekäs (née Lehmus), O.
Design of high-efficiency antennas for mobile communications devices, August 2005

S 273 Laitinen, T.
Advanced spherical antenna measurements, December 2005

S 274 Salonen, I., Icheln, C., Vainikainen, P.
Beamforcing with wide null sectors for realistic arrays using directional weighting, December 2005

S 275 Räisänen, A.V., Lindberg, S.
TKK Radio Laboratory research and education 2005, March 2006

S 276 Salonen, I.
Evaluation and compensation of mutual coupling and other non-idealities in small antenna arrays, May 2006

S 277 Suvikunnas, P., Salo, J., Vuokko, L. Kivinen, J., Sulonen, K., Vainikainen, P.
Comparison of MIMO antenna configurations: Methods and experimental results, June 2008

S 278 Salo, J.
Statistical analysis of the wireless propagation channel and its mutual information, July 2006

ISBN 951-22-8296-8I
ISSN 1456-3835